

# The cost of toxin production in phytoplankton: the case of PST producing dinoflagellates

**Chakraborty, Subhendu; Mohr, Marina; Andersen, Ken Haste; Kiørboe, Thomas**

*Published in:*
I S M E Journal

*Link to article, DOI:*
10.1038/s41396-018-0250-6

*Publication date:*
2019

*Document Version*
Early version, also known as pre-print

**Title of the paper: The cost of toxin production in phytoplankton: the case of PST producing dinoflagellates**

**Running title: Cost of toxin production**

Subhendu Chakraborty[†], Marina Pančić, Ken H. Andersen, Thomas Kiørboe

Centre for Ocean Life, DTU Aqua, Technical University of Denmark, Kemitorvet, 2800 Kgs. Lyngby, Denmark

[†]Corresponding author: Building 202, Centre for Ocean Life, DTU Aqua, Technical University of Denmark, Kemitorvet, 2800 Kgs. Lyngby, Denmark. Tel: +4591714664. Email: subc@aqua.dtu.dk

## Abstract

Many species of phytoplankton produce toxins that may provide protection from grazing. In that case one would expect toxin production to be costly; else all species would evolve toxicity. However, experiments have consistently failed to show any costs. Here, we show that costs of toxin production are environment dependent but can be high. We develop a fitness optimization model to estimate rate, costs, and benefits of toxin production, using PST (paralytic shellfish toxin) producing dinoflagellates as an example. Costs include energy and material (nitrogen) costs estimated from well-established biochemistry of PSTs, and benefits are estimated from relationship between toxin content and grazing mortality. The model reproduces all known features of PST production: inducibility in the presence of grazer cues, low toxicity of nitrogen-starved cells, but high toxicity of P- and light-limited cells. The model predicts negligible reduction in cell division rate in nitrogen replete cells, consistent with observations, but >20% reduction when nitrogen is limiting and abundance of grazers high. Such situation is characteristic of coastal and oceanic waters during summer when blooms of toxic algae typically develop. The investment in defense is warranted, since the net growth rate is always higher in defended than in undefended cells.



## Key words

Defense; Trade-off; Environment-dependent cost

## Introduction

Many phytoplankton species produce substances that are toxic to humans, hence we consider such phytoplankton 'toxic algae', but the evolution and functional role of these secondary metabolites remain unclear. They may be released into the environment and have allelochemical effects to combat competitors [1, 2] or grazers [3], they may be mainly intracellular and have toxic and/or deterrent effects on grazers [4, 5], or in mixotrophic species they may have offensive roles, functioning as a venom towards prey [6–8]. Some toxic algae may also form dense blooms, potentially promoted by their toxicity and consequent grazer deterrent effects, and a defensive role of toxin production is thus often assumed [4, 9]. This interpretation is supported by the observations that algal toxins often have a deterrent rather than a toxic effect on grazers [10–15], and that toxin production may be upregulated in the presence of grazers or their cues, as demonstrated in dinoflagellates, *Alexandrium* spp. [13, 16, 17], and in diatoms, *Pseudo-nitzschia* spp. [18]. The latter observation also suggests that toxin production comes at a cost – why else regulate the production in response to the need? Optimal defense theory, well founded in terrestrial plant ecology, predicts that inducibility of defense should evolve only when the defense is costly and variable in time [19]. However, experiments have generally been unable to demonstrate such costs in toxic phytoplankton, and the growth rates of grazer-induced and un-induced cells, or of toxic and nontoxic strains of the same phytoplankton species appear to be similar [3, 13, 16, 18], and model exercises have similarly suggested costs to be trivial [20]. However, if defense via toxin production is both effective and costless, one would expect most phytoplankton to be toxic, which is far from being the case [19]. Also, the promotion of phytoplankton diversity in the ocean due to grazing and consequent evolution of defense mechanisms, as demonstrated in

both theoretical models and considerations [21–23] and whole-community experiments [24], functions only if the defense comes at a cost.

One of the most studied groups of toxic phytoplankton is the dinoflagellate *Alexandrium* spp. since the toxins it produces, Paralytic Shellfish Toxins (PSTs), have serious effects on humans. The main potential grazers of dinoflagellates are copepods. While the toxin production may be induced by grazer (copepod) cues [13], the production also depends on the nutrient status of the algae. Specifically, when nitrogen or carbon (light) is limiting the PST production is reduced, while nutrient balanced or P-limited cells may produce PSTs at a high rate (growth of P-limited cells decreases while the production of toxins continues) [25, 26]. PSTs contain large amounts of nitrogen, and so this dependency suggests that the costs of PST production only become obvious when N or light is limiting, and may become manifest either as a reduction in growth rate because part of the assimilated N goes towards PST production; or as a cessation of the production of PSTs in favor of a higher growth rate with a consequent loss of the defense; or a combination of the two.

Here, we explore by means of a simple resource allocation model the costs of chemical defense in phytoplankton, using PST producing dinoflagellate *Alexandrium* spp. as an example. We consider both energy and material costs of PST production, their dependency on environmental conditions, and the reduction in mortality that is achieved by the defense investments. Through fitness optimization we demonstrate that costs can be substantial, leading to > 20% reduction in cell division rate, when grazer abundance is high and nitrogen availability is low. We also examine the conditions under which the production of toxins provides maximum benefit to the toxin producing species.

**Model description:**

The model is based on a resource allocation optimization model modified from Berge *et al.* [27]. The division rate of phytoplankton depends on the acquisition of three resources, viz. carbon (via photosynthesis), nitrogen (as nitrate), and phosphorous (as phosphate), as well as on metabolic expenses. The cells may invest some of their assimilated nitrogen into toxin production and combust some of their fixed organic carbon to cover costs of toxin synthesis, and in return experience reduced grazing mortality. We search for the investment that maximizes the fitness of the cells, defined as the difference between cell division rate and mortality rate (= net growth rate). We use the model to explore the dependency of division rate, net growth rate, and toxicity on the environmental resource availability and predation risk.

Uptake of carbon, nitrogen and phosphorous to the cell is described by the symbol $J_i$ (mass flows $i$ being carbon via light-dependent photosynthesis (C), nitrogen (N) or phosphorous (P) in units of $\mu$g per day; see Table 1 for central symbols and parameters), and are combined to synthesize new biomass (Fig. 1). Respiratory costs, $R_C$ (units of µg C per day), include costs of biomass synthesis (incl. transport) and maintenance of the structure. Toxin is produced at a rate, $T_r$, and implies an additional respiratory cost, $R_T$. Biomass synthesis rate, $J_{tot}$, is constrained by the stoichiometric balance between carbon, nitrogen and phosphorous. Finally, we assume that toxins and structure have constant but different stoichiometry.

*Uptake of carbon, nitrogen, and phosphorous*

The potential uptake $J_i$ of resource $i$ ($C$, N, $P$) is governed by a standard saturating functional response:

$$J_i = M_i \frac{A_i Y_i}{A_i Y_i + M_{\mathrm{i}}}, (1)$$

where $A_i$ is the affinity for resource *i*, $Y_i$ resource concentration ($\mu$g $L^{-1}$), and $M_i$ is the maximum uptake rate.

*Costs*

Respiratory costs include costs of both uptake and mobilization of resources for synthesis through each pathway, and the maintenance of the structure. This metabolic cost is assumed to be 30% of the total carbon budget [28] plus a constant basal respiration ($R_0$) independent of $J_C$, i.e.,

$$R_C = 0.3J_C + R_0. \ (2)$$

*Rate and cost of toxin production*

Let $\theta$ be the fraction of nitrogen uptake that a toxic phytoplankton cell devotes to toxin production. Then the potential rate of toxin production is (units of $\mu$g N $d^{-1}$):

$$T_{pot}(\theta) = \theta J_N. \qquad (3)$$

As the toxin production needs carbon both for building the toxin molecules and to fuel the respiratory costs of toxin production, the actual toxin production rate may be limited by the available carbon to:

$$T_r(\theta) = \min\left[T_{pot}(\theta), (J_C - R_C)/(n_T + r_T)\right], \ (4)$$

where $n_T$ is the mass of carbon need per mass of nitrogen in the toxin, and $r_T$ is the respiratory cost per nitrogen synthesized into toxins (units of g C (g N) $^{-1}$).

The total cost of toxin production in terms of carbon then becomes ($\mu$g C $d^{-1}$):

$$R_T(\theta) = (n_T + r_T)T_r(\theta). \quad (5)$$

*Synthesis and growth rate*

The assimilated carbon, nitrogen and phosphorous are combined to synthesize new structure. We assume constant C:N mass ratio, $Q_{CN}$ (units of $\mu$g C ($\mu$g N)$^{-1}$) and C:P mass ratio, $Q_{CP}$ (units of $\mu$g C ($\mu$g P)$^{-1}$) of the cell. The total available carbon for growth is then $J_C - R_C - R_T$ where $J_C$ represents the total uptake of carbon through photosynthesis, and $R_C$ and $R_T$ represent the costs of maintenance and biomass synthesis, and costs of toxin production, respectively. The carbon required to synthesize biomass from nutrients is $Q_{CN}(J_N - T_r)$ and $Q_{CP}J_P$ for nitrate and phosphate, respectively. The growth rate is constrained by the limiting resource (Liebig's law of the minimum) such that the total flux of carbon (and nutrients) available for growth $J_{\mathrm{tot}}$ is:

$$J_{\mathrm{tot}}(\theta) = \min[J_C - R_C - R_T(\theta),\ Q_{CN}(J_N - T_r(\theta)),\ Q_{CP}J_P]. \quad (6)$$

Synthesis is not explicitly limited by a maximum synthesis capacity; limitation of synthesis is taken care of by the limitation of uptake of carbon, nitrogen and phosphorous in the functional responses (Eq. 1). The division rate $\mu$ of the cells ($d^{-1}$) is the total flux of carbon divided by the carbon mass of the cell ($w_X$):

$$\mu(\theta) = J_{\mathrm{tot}}(\theta)/w_X. \quad (7)$$

Further subtracting the predation mortality ($m_p$) yields the net growth rate ($r$):

$$r(\theta) = \mu(\theta) - m_p(\theta). \quad (8)$$

We assume that predation mortality increases linearly with zooplankton biomass ($Z$), and due to the toxin production, zooplankton reduces its grazing pressure on toxic cells exponentially as:

$$m_p(\theta) = m_{p,0} Z e^{-\beta T(\theta)}, \quad (9)$$

where $m_{p,0}$ is a mortality constant, $T$ is the cellular toxin content ($\mu$g N cell$^{-1}$) estimated as the toxin production rate divided by the cell division rate ($= T_r/\mu$), and $\beta$ represents the strength of toxic effect.

The resulting population growth rate, $r(\theta)$, is a measure of the fitness of the phytoplankton and we assume that the cell has the ability to optimize its growth rate by regulating its resource allocation to toxin production such that it maximizes its fitness. The optimal proportion of assimilated N devoted to toxin production then becomes:

$$\theta^* = \underset{\theta}{\operatorname{argmax}}\{r(\theta)\}. \quad (10)$$

**Model parameterization**

Calibration of parameters is based on laboratory measurements on the dinoflagellates *Alexandrium minutum* and *A. tamarense* as the toxic species, and the copepods *Acartia clausi* and *A. tonsa* as the grazer zooplankton. To calibrate the basic grazing parameters, we use data for non-toxic strains of *A. minutum.*

*Parameters related to phytoplankton division rate ($\mu$):*

We use experimental observations reported in the literature for cell division rate ($\mu$) of *A. minutum* as a function of light intensity (L) and nutrient concentrations (N and

P) to estimate parameter values for maximum uptake rates ($M_i$) and affinities ($A_i$) (Fig. 2a-c). While calibrating these parameters a non-toxic strain of *A. minutum* was considered, and as a result, no cost is deducted. For calibration, we adjust the parameters manually to fit the curves with data and keep them close to the existing values of the parameters from other studies (when available). Due to Liebig's minimum law for synthesis (eq. 6), the synthesis is limited by one of the resources (either C or N) and further growth cannot materialize in spite of the availability of other non-limiting resource. As a result, growth cannot increase any further.

We use a constant value $1.07\times 10^{-4}$ $\mu$g C $d^{-1}$ for the basal respiration rate ($R_0$) taken from the range reported in Frangoulis *et al.* [29].

*Parameters related to the cost of toxin production:*

To estimate the two parameters related to the cost of toxin production ($n_T$, $r_T$), we consider the stoichiometry of PSTs and the biochemistry of PST synthesis. PSTs produced by *Alexandrium* spp. (and other organisms) consist of saxitoxin and multiple derivatives; they are cyclic nitrogenous compounds that are synthesized from amino acid precursors. Here we consider the synthesis of saxitoxin, one of the dominating toxins, from the amino acid glutamate via arginine to estimate the approximate costs of toxin production. The costs are two-fold; i.e. the metabolic cost of biosynthesis, $r_T$, and the cost in terms of material invested in the toxin, $n_T$.

*Material investment* ($n_T$): The molecular formula of saxitoxin in $C_{10}H_{17}N_70_4$, that is 10 moles of carbon per 7 moles of nitrogen, or $n_T$ = (10x12)/(7x14) = 1.23 $\mu$g C ($\mu$g N)$^{-1}$.

194 *Metabolic expenses* ($r_T$): Saxitoxin is synthesized from arginine [30], which in turn is
195 typically synthesized from glutamate that in phytoplankton has to be synthesized *de*
196 *novo*. The metabolic cost of converting glutamate to arginine is 12 mol ATP per mol
197 of arginine, and the synthesis of arginine precursors (i.e. glutamate and carbamoyl-P)
198 requires another 32 mol of ATP, i.e. a total of 44 mol ATP per mol of arginine [31].
199 We have no estimate of the cost of synthesizing saxitoxin from arginine (e.g.,
200 necessary transcripts and translation to enzymes) as well as costs due to actual or
201 potential autotoxicity (hence we ignore it), but it takes 3 mol of arginine to synthesize
202 one mol of saxitoxin. Therefore, it requires at least 132 mol of ATP to synthesize 1
203 mol of saxitoxin. The respiratory equivalent of ATP synthesis is about 0.235 mol ATP
204 synthesized per liter of oxygen consumed; or about 2 g of organic carbon combusted
205 per mol of ATP synthesized [32]. Thus, 2x132 g of organic carbon is respired per mol
206 of toxin synthesized. With 7x14 g N per mol toxin yields an estimate of $r_T$= 2.7 $\mu$g C
207 ($\mu$g N)$^{-1}$.

208 *Parameters related to zooplankton feeding:*

209 The parameters related to reduction in feeding on toxic cell ($\beta$) was calibrated from
210 Teegarden & Cembella [12] who quantified the feeding rate on a toxic strain of *A.*
211 *minutum* by *A. tonsa* as a function of cellular toxin content ($\mu$g N cell$^{-1}$). We fit Eq. 9
212 to the experimental data to estimate $\beta$ (Fig. 2d). We use 8.95$\times 10^{-4}$ $\mu$g C as the
213 cellular carbon content of *A. minutum* [28], and chose the value of the mortality
214 constant ($m_{p,0}$) as 0.008 L ($\mu$g C)$^{-1}$ d$^{-1}$ based on the clearance rate of *A. tonsa* [34].

215

216 **Results**

*Optimal allocation strategy*

The optimal allocation of nitrogen to toxin production is the one that yields the highest population growth rate (Fig. 3). The optimal allocation of N to toxin production increases with decreasing environmental nitrogen availability and increasing concentration of zooplankton (Fig. 3). As a result, the investment in defense - toxin production - in toxic dinoflagellates varies with both N-availability and grazing pressure, with implications to cell division rate, grazing mortality rate, and population growth rate (Fig. 4, Fig. 5, Fig. 6 and Fig. 7).

*Toxin production, grazing mortality, and cost of defense*

At high N concentrations, the cells produce toxin whenever zooplankton is present but production ceases in the absence of grazers (Fig. 4a). Note that for simplicity we assume that toxin production rate becomes zero when there is no grazer. In contrast, at low N, phytoplankton produce toxins only when zooplankton biomass exceeds a threshold concentration, and the cellular toxin content increases with the biomass of the zooplankton (Fig. 4a, 6b).

Defended cells experience lower grazing mortality than undefended cells especially when nitrogen availability is high and zooplankton concentration is low (Fig. 4d) as cellular toxin content remains high (Fig. 4a). Taken together the grazing mortality increases with zooplankton density and decreases with availability of nitrogen.

The cost of the defense can be quantified as a reduction in the cell division rate of defended relative to undefended cells. This cost is significant only at high zooplankton biomass and/or low nitrogen availability (Fig. 4b, Fig. 5a) and increases with increasing zooplankton biomass and decreasing nitrogen concentration (Fig. 6c,

d). At realistically high zooplankton biomass and realistically low nitrogen availability, cell division rate may be reduced by more than 20%. At high nitrogen concentrations, the cells produce toxins from the excess nitrogen (not used for growth) and therefore the costs are, of course, unmeasurably low (Fig. 6d).The net outcome of the defense investment is that defended cells have similar or higher population growth rates (fitness) than undefended cells under all nutrient conditions (Fig. 4c). The absolute enhancement is largest at high N (Fig. 6e) whereas the relative advantage is most pronounced at low N and high zooplankton biomass (Fig. 6f).

*Effects of P and light limitation*

If phosphate or light rather than nitrogen limit cell growth, N is in excess and the excess N can be allocated to toxin production and the cells consequently become well defended. Figs. 7a and b display the effects of light limitation on toxin production and cellular toxin contents, respectively. There are two regions in this parameter space: the left region where light is limiting and toxin production increases with light intensity while toxin content decreases with light intensity; and the right region, where nitrogen is limiting and both toxin production and cellular toxin content are independent of light intensity. Toxin production and cellular contents similarly vary in the nitrogen-phosphorous parameter space, between phosphorous limitation at low P and nitrogen limitation at high P (Fig. 7c, d). Under all conditions, cellular toxin contents increase with decreasing ambient P.

*Sensitivity analysis of $\beta$ and $r_T$*

Since the parameter $\beta$ was calibrated based on only four available data points (Figure 2d), we perform a sensitivity analysis by varying $\beta$, which represents the reduction in

zooplankton grazing due to cellular toxin (see supplementary material fig. A1). Overall, the qualitative patterns described above are robust to changes in $\beta$. When nitrogen concentrations are high, there is no observable change in cellular toxin concentration with varying $\beta$ as organisms produce toxins at their maximum rate and consequently division rates remain same. However, due to the increase in predation pressure with decreasing $\beta$, population growth rate decreases. On the other hand, with decrease in nitrogen concentrations, organisms produce more toxin with decrease in $\beta$, leading to reduction in division rates as well as growth rates.

Similarly, varying the parameter $r_T$, representing the metabolic cost of synthesizing toxin, does not lead to observable changes in the system dynamics (see supplementary material fig. A2).

## Discussion

Experiments have demonstrated that PST producing dinoflagellates become less toxic when N-starved, that toxin content is high in exponentially growing cells in N:P balanced environments, and that the cells become most toxic when P-limited [20, 26, 35–37]. Light-limited cells also accumulate more toxins [38] and toxin production is enhanced in the presence of grazer cues [13]. Our model qualitatively reproduces all these observations.

The model further conforms with the experimental observation that the cost of toxin production, quantified as a reduction in cell division rate of toxin-producing cells compared to cells or strains that produce less or no toxins, is negligible when resources, mainly N and light, are plentiful [3, 13]. However, when light or nitrogen are limiting cell growth, and when grazers are abundant, we predict that the cost of

286 investing in toxin production may be substantial and lead to > 20% reduction in cell
287 division rate. There is evidence for other defense mechanisms in phytoplankton where
288 the cost of the defense only materializes when resources are limiting [39–41].
289 However, the prediction of costs of toxin production still remains to be tested
290 experimentally. The costs of the investment are two-fold: (i) the cells need nitrogen to
291 build toxin molecules, and this requirement compete with the nitrogen investment in
292 cell structure and growth. While the nitrogen requirement for toxin production is
293 small in absolute terms, leading John and Flynn [20] to consider it trivial, it becomes
294 significant when nitrogen is limiting, and may eventually lead to a total shut down of
295 toxin production. (ii) The cells further need energy for the synthesis of toxins, and this
296 energy eventually comes from photosynthesis. This is why toxin production rate
297 increases with light intensity when light is the limiting resource. In this situation, cell
298 division rate increases faster than toxin production rate with increasing light, and
299 therefore cellular toxin content decreases with increasing light, an effect and a
300 mechanism in agreement with experimental observations [38].

301 The environmental conditions that promote cell toxicity, i.e., high grazer biomass,
302 actually coincide with the time of the year when nitrogen is the most limiting resource
303 in temperate shelf regions. Thus, zooplankton (copepod) biomass is at its seasonal
304 maximum during summer and may easily exceed 10-100 $\mu$g C $L^{-1}$ [42], which will
305 impose a high predation mortality and thus induce high cell toxicity. At this time of
306 the year, concentrations of inorganic nitrogen in surface waters in temperate shelf
307 regions are low, typically below 1-10 $\mu$g N $L^{-1}$ [43, 44], and under these conditions
308 the model predicts that the cost of toxin production is substantial, leading to > 20%
309 decrease in cell division rate. However, the investment in defense pays off since
310 defended cells experience lower grazing mortality, and may consequently have net

311 growth rates up to twice or more of that of undefended cells (e.g. Fig. 6f). If the toxins
312 have deterrent rather than toxic effects, i.e., preventing the toxic cells from being
313 consumed rather than killing grazers that do consume the cells [10, 11, 45], then the
314 toxic cells may have a competitive advantage and a monospecific bloom may
315 develop. Indeed, blooms of toxic algae typically occur during summer [46], which is
316 consistent with these considerations.

317 Furthermore, the toxic species can also gain growth advantage under high nitrogen
318 and high grazer biomass, as growth rates can be doubled due to the benefit provided
319 by toxin production at a negligible production cost (Fig. 6d, f). Such situations are
320 comparable with many coastal areas where N:P ratios remain considerably high due
321 to erratic input of nitrogen from human activities, and can consequently result in toxic
322 blooms [47]. Thus, potentially toxic species can also become toxic when exposed to
323 high N regime caused by eutrophication.

324 The success of toxic bloom formation also depends on the evolutionary history of
325 zooplankton grazer and toxic species [40]. Evidence from both fresh- and marine
326 waters shows that grazers can evolve full or partial resistance against the toxic algae
327 [48, 49]. Our results suggest that cellular toxin content will increase in the presence of
328 toxin-resistant grazers as will the costs (see supplementary material fig. A1).
329 However, if the benefits in terms of reduced grazing mortality vanish due to grazer
330 resistance, the possibility of success of the toxic species in terms of forming bloom
331 will be reduced or disappear.

332 Many phytoplankton species have evolved what is supposed to be defense
333 mechanisms to avoid or reduce predation, ranging from hard shells and spines, to
334 evasive behaviors and toxin production, and such defenses may have significant

implications on predator-prey interactions, population dynamics, and diversity of phytoplankton communities [50]. However, the trade-offs are rarely quantified and often not even documented. While there is increasing evidence that toxin-production in many cases provides partial protection from grazing in dinoflagellates, the costs have hitherto not been properly quantified. The currencies of benefits and costs are growth and mortality. Here, we have shown that the costs are not only strongly dependent on the concentration of grazers but also on the resource availability, and that the realized costs in nature are typically highest during summer when the defense is most needed. The delicate balance between costs, benefits, and resource availability not only explains why the defense is inducible but also has implications for the timing of toxic algal blooms. Further studies on costs and benefits of toxin production are needed to experimentally test our model predictions (e.g., toxin production and growth under sufficient and deficient resources), and for deeper understanding of the mechanisms and evolution of inducible toxin production. At present, very little is known about the consequences of inducible toxin production on the community level in complex communities. Future work should be devoted towards investigating the complex integrated ecological issues of inducible toxin production, species diversity, and food web structure.

**Acknowledgments**

The Centre for Ocean Life is supported by the Villum Foundation. S.C. was supported by the H. C. Ørsted COFUND postdoc fellowship and additional support was received from the Gordon & Betty Moore Foundation through award #5479.

**Conflict of interest**

The authors declare that they have no conflict of interest.

## References


1. Blossom HE, Andersen NG, Rasmussen SA, Hansen PJ. Stability of the intra- and extracellular toxins of Prymnesium parvum using a microalgal bioassay. *Harmful Algae* 2014; **32**: 11–21.

2. Legrand C, Rengefors K, Fistarol GO, Granéli E. Allelopathy in phytoplankton - biochemical, ecological and evolutionary aspects. *Phycologia* 2003; **42**: 406–419.

3. John U, Tillmann U, Hülskötter J, Alpermann TJ, Wohlrab S, Van De Waal DB. Intraspecific facilitation by allelochemical mediated grazing protection within a toxigenic dinoflagellate population. *Proc R Soc B Biol Sci* 2015; **282**: 1–9.

4. Turner JT. Planktonic marine copepods and harmful algae. *Harmful Algae* 2014; **32**: 81–93.

5. Colin SP, Dam HG. Effects of the toxic dinoflagellate Alexandrium fundyense on the copepod Acartia hudsonica: A test of the mechanisms that reduce ingestion rates. *Mar Ecol Prog Ser* 2003; **248**: 55–65.

6. Driscoll WW, Hackett JD, Ferrière R. Eco-evolutionary feedbacks between private and public goods: Evidence from toxic algal blooms. *Ecol Lett* 2016; **19**: 81–97.

7. Blossom HE, Daugbjerg N, Hansen PJ. Toxic mucus traps: A novel mechanism that mediates prey uptake in the mixotrophic dinoflagellate Alexandrium pseudogonyaulax. *Harmful Algae* 2012; **17**: 40–53.

8. Sheng J, Malkiel E, Katz J, Adolf JE, Place AR. A dinoflagellate exploits toxins to immobilize prey prior to ingestion. *Proc Natl Acad Sci* 2010; **107**: 2082–2087.

9. Wolfe G V. The chemical defense ecology of marine unicellular plankton: Constraints, mechanisms, and impacts. *Biol Bull* 2000; **198**: 225–244.

10. Xu J, Nielsen LT, Kiørboe T. Foraging response and acclimation of ambush feeding and feeding-current feeding copepods to toxic dinoflagellates. *Limnol Oceanogr* 2018.

11. Xu J, Hansen JP, Nielsen TL, Krock B, Tillmann U, Kiørboe T. Distinctly different behavioral responses of a copepod, Temora longicornis, to different strains of toxic dinoflagellates, Alexandrium spp. *Harmful Algae* 2017; **62**: 1–9.

12. Teegarden GJ, Cembella AD. Grazing of toxic dinoflagellates, Alexandrium spp, by adult copepods of coastal Maine: Implications for the fate of paralytic shellfish toxins in marine food webs. *J Exp Mar Bio Ecol* 1996; **196**: 145–176.

13. Selander E, Thor P, Toth G, Pavia H. Copepods induce paralytic shellfish toxin production in marine dinoflagellates. *Proc R Soc B Biol Sci* 2006; **273**: 1673–1680.

14. Schultz M, Kiørboe T. Active prey selection in two pelagic copepods feeding on potentially toxic and non-toxic dinoflagellates. *J Plankton Res* 2009; **31**: 553–561.

15. Sykes PF, Huntley ME. Acute physiological reactions of Calanus pacificus to

selected dinoflagellates: Direct observations. *Mar Biol* 1987; **94**: 19–24.

16. Selander E, Fagerberg T, Wohlrab S, Pavia H. Fight and flight in dinoflagellates? Kinetics of simultaneous grazer-induced responses in Alexandrium tamarense. *Limnol Oceanogr* 2012; **57**: 58–64.

17. Senft-Batoh CD, Dam HG, Shumway SE, Wikfors GH. A multi-phylum study of grazer-induced paralytic shellfish toxin production in the dinoflagellate Alexandrium fundyense: A new perspective on control of algal toxicity. *Harmful Algae* 2015; **44**: 20–31.

18. Harðardóttir S, Pančić M, Tammilehto A, Krock B, Møller EF, Nielsen TG, et al. Dangerous relations in the Arctic marine food web: Interactions between toxin producing Pseudo-nitzschia diatoms and Calanus copepodites. *Mar Drugs* 2015; **13**: 3809–3835.

19. Karban R. The ecology and evolution of induced resistance against herbivores. *Funct Ecol* 2011; **25**: 339–347.

20. John EH, Flynn KJ. Modelling changes in paralytic shellfish toxin content of dionoflagellates in response to nitrogen and phosphorus supply. *Mar Ecol Prog Ser* 2002; **225**: 116–147.

21. Thingstad TF, Våge S, Storesund JE, Sandaa R-A, Giske J. A theoretical analysis of how strain-specific viruses can control microbial species diversity. *Proc Natl Acad Sci* 2014; **111**: 7813–7818.

22. Våge S, Storesund JE, Giske J, Thingstad TF. Optimal defense strategies in an idealized microbial food web under trade-off between competition and defense.

*PLoS One* 2014; **9**.

23. Strauss SY, Rudgers JA, Lau JA, Irwin RE. Direct and ecological costs of resistance to herbivory. *Trends Ecol Evol* 2002; **17**: 278–285.

24. Leibold MA, Hall SR, Smith VH, Lytle DA. Herbivory enhances the diversity of primary producers in pond ecosystems. *Ecology* 2017; **98**: 48–56.

25. Anderson DM, Kulis DM, J.J. S, Hall S, Lee C. Dynamics and physiology of saxitoxin production by the dinoflagellate Alexandrium spp. *Mar Biol* 1990; **104**: 511–524.

26. John EH, Flynn KJ. Growth dynamics and toxicity of Alexandrium fundyense (Dinophyceae): The effect of changing N:P supply ratios on internal toxin and nutrient levels. *Eur J Phycol* 2000; **35**: 11–23.

27. Berge T, Chakraborty S, Hansen PJ, Andersen KH. Modeling succession of key resource-harvesting traits of mixotrophic plankton. *ISME J* 2017; **11**: 212–223.

28. López-Sandoval DC, Rodríguez-Ramos T, Cermeño P, Sobrino C, Marañón E. Photosynthesis and respiration in marine phytoplankton: Relationship with cell size, taxonomic affiliation, and growth phase. *J Exp Mar Bio Ecol* 2014; **457**: 151–159.

29. Frangoulis C, Carlotti F, Eisenhauer L, Zervoudaki S. Converting copepod vital rates into units appropriate for biogeochemical models. *Prog Oceanogr* 2010; **84**: 43–51.

30. Kellmann R, Mihali TK, Young JJ, Pickford R, Pomati F, Neilan BA.

Biosynthetic intermediate analysis and functional homology reveal a saxitoxin gene cluster in cyanobacteria. *Appl Environ Microbiol* 2008; **74**: 4044–4053.

31. Atkinson DE. Cellular Energy Metabolism and Its Regulation. 1977. Academic Press.

32. Kiørboe T, Møhlenberg F, Hamburger K. Bioenergetics of the planktonic copepod Acartia tonsa: Relation between feeding, egg production and respiration, and composition of specific dynamic action. *Mar Ecol Prog Ser* 1985; **26**: 85–97.

34. Saiz E, Kiørboe T. Predatory and suspension feeding of the copepod Acartia tonsa in turbulent environments. *Mar Ecol Prog Ser* 1995; **122**: 147–158.

35. Boyer GL, Sullivan JJ, Andersen RJ, Harrison PJ, Taylor FJR. Effects of nutrient limitation on toxin production and composition in the marine dinoflagellate Protogonyaulax tamarensis. *Mar Biol* 1987; **128**: 123–128.

36. Han M, Lee H, Anderson DM, Kim B. Paralytic shellfish toxin production by the dinoflagellate Alexandrium pacificum (Chinhae Bay, Korea) in axenic, nutrient-limited chemostat cultures and nutrient-enriched batch cultures. *Mar Pollut Bull* 2016; **104**: 34–43.

37. Murata A, Nagashima Y, Taguchi S. N:P ratios controlling the growth of the marine dinoflagellate Alexandrium tamarense: Content and composition of paralytic shellfish poison. *Harmful Algae* 2012; **20**: 11–18.

38. Ogata T, Ishimura T, Kodama M. Effect of water temperature and light intensity on growth rate and toxicity change in Protogonyaulax tamarensis.

*Mar Biol* 1987; **95**: 217–220.

39. Zhu X, Wang J, Chen Q, Chen G, Huang Y, Yang Z. Costs and trade-offs of grazer-induced defenses in Scenedesmus under deficient resource. *Sci Rep* 2016; **6**: 1–10.

40. Yoshida T, Hairston NG, Ellner SP. Evolutionary trade-off between defence against grazing and competitive ability in a simple unicellular alga, Chlorelia vulgaris. *Proc R Soc B-Biological Sci* 2004; **271**: 1947–1953.

41. Yoshida T, Jones LE, Ellner SP, Fussmann GF, Hairston NG. Rapid evolution drives ecological dynamics in a predator – prey system. *Nature* 2003; **424**: 303–306.

42. Kiørboe T, Nielsen TG. Regulation of zooplankton biomass and production in a temperate, coastal ecosystem. 1. Copepods. *Limnol Ocean* 1994; **39**: 493–507.

43. Andersson L. Trends in nutrient and oxygen concentrations in the Skagerrak-Kattegat. *J Sea Res* 1996; **35**: 63–71.

44. Brockmann UW, Topcu DH. Nutrient atlas of the central and northern North Sea. 2002. Federal Environmental Agency, Berlin, Germany.

45. Teegarden GJ. Copepod grazing selection and particle discrimination on the basis of PSP toxin content. *Mar Ecol Prog Ser* 1999; **181**: 163–176.

46. Heisler J, Glibert PM, Burkholder JM, Anderson DM, Cochlan W, Dennison WC, et al. Eutrophication and harmful algal blooms: A scientific consensus. *Harmful Algae* 2008; **8**: 3–13.

47. Hallegraeff GM. A review of harmful algal blooms and their apparent global increase. *Phycologia* 1993; **32**: 79–99.

48. Gilbert JJ. Differential effects of Anabaena affinis on Cladocerans and Rotifers: Mechanisms and implications. *Ecology* 1990; **71**: 1727–1740.

49. Colin SP, Dam HG. Latitudinal differentiation in the effects of the toxic dinoflagellate Alexandrium spp. on the feeding and reproduction of populations of the copepod Acartia hudsonica. *Harmful Algae* 2002; **1**: 113–125.

50. Pančić M, Kiørboe T. Phytoplankton defence mechanisms: Traits and trade-offs. *Biol Rev* 2018.

51. Redfield AC. The biological control of chemical factors in the environment. *Am Sci* . 1958. Sigma Xi, The Scientific Research Honor Society. , **46**: 205–221

52. Chang FH, McClean M. Growth responses of Alexandrium minutum (Dinophyceae) as a function of three different nitrogen sources and irradiance. *New Zeal J Mar Freshw Res* 1997; **31**: 1–7.

53. Ignatiades L, Gotsis-Skretas O, Metaxatos A. Field and culture studies on the ecophysiology of the toxic dinoflagellate Alexandrium minutum (Halim) present in Greek coastal waters. *Harmful Algae* 2007; **6**: 153–165.

54. Lim PT, Leaw CP, Usup G, Kobiyama A, Koike K, Ogata T. Effects of light and temperature on growth, nitrate uptake, and toxin production of two tropical dinoflagellates: Alexandrium tamiyavanichii and Alexandrium minutum

(Dinophyceae). *J Phycol* 2006; **42**: 786–799.

530 **Table 1.** Central symbols and general parameters. Index $i$ refers to carbon ($C$) via
531 light-dependent photosynthesis where light intensity is measured in units of
532 $\mu$E $m^{-2}s^{-1}$, nitrogen ($N$) in units of $\mu$g N $L^{-1}$ or phosphorous (P) in units of $\mu$g P $L^{-1}$.
533 Calibration of parameters is based on data from laboratory measurements and
534 provided in the 'Model parameterization' section.

| Symbol | Description | Value | Unit | Reference |
|---|---|---|---|---|

| | | | | |
|---|---|---|---|---|
| L | Light flux in the environment | - | $\mu$E $m^{-2}s^{-1}$ | - |
| N | Concentration of nitrogen in the environment | - | $\mu$g N $L^{-1}$ | - |
| P | Concentration of phosphorous in the environment | - | $\mu$g P $L^{-1}$ | - |
| $w_X$ | Cellular mass of toxic algae | $8.95 \times 10^{-4}$ | $\mu$g C | [28] |
| Z | Biomass of zooplankton | - | $\mu$g C $L^{-1}$ | - |
| | **Functional responses** | | | |
| $J_i$ | Flux of assimilated substance | | $\mu$g C $d^{-1}$, $\mu$g N $d^{-1}$, or $\mu$g P $d^{-1}$ | Eq. (1) |
| $A_L$ | Affinity for light | $3.1 \times 10^{-5}$ | $\mu$g C ($\mu$E $m^{-2}s^{-1}$)$^{-1}$ $d^{-1}$ | Calibrated |
| $A_N$ | Affinity for nitrogen | $3 \times 10^{-6}$ | L $d^{-1}$ | Calibrated |
| $A_P$ | Affinity for phosphorous | $3 \times 10^{-7}$ | L $d^{-1}$ | Calibrated |
| $M_L$ | Max. uptake rate of C through photosyntehsis | $9.5 \times 10^{-4}$ | $\mu$g C $d^{-1}$ | Calibrated |
| $M_N$ | Max. uptake rate of N | $1.1 \times 10^{-4}$ | $\mu$g N $d^{-1}$ | Calibrated |
| $M_P$ | Max. uptake rate of P | $1.3 \times 10^{-5}$ | $\mu$g P $d^{-1}$ | Calibrated |
| | **Costs and toxin production** | | | |
| $R_C$ | Total metabolic cost | - | $\mu$g C $d^{-1}$ | Eq. (2) |
| $R_0$ | Basal respiration rate | $1.07 \times 10^{-4}$ | $\mu$g C $d^{-1}$ | [29] |
| $\theta$ | Fraction of N devoted to toxin | - | - | Eq. (10) |
| $T_{pot}$ | Potential toxin production rate | - | $\mu$g N $d^{-1}$ | Eq. (3) |
| $T_r$ | Actual toxin production rate | - | $\mu$g N $d^{-1}$ | Eq. (4) |
| T | Cellular toxin content | - | $\mu$g N $cell^{-1}$ | - |
| $R_T$ | Cost of toxin production | - | $\mu$g C $d^{-1}$ | Eq. (5) |
| $n_T$ | Material cost of toxin production | 1.23 | $\mu$g C ($\mu$g N)$^{-1}$ | Calibrated |
| $r_T$ | Metabolic cost of synthesizing toxin | 2.7 | $\mu$g C ($\mu$g N)$^{-1}$ | Calibrated |
| | **Predation** | | | |
| $m_p$ | Predation mortality | - | $d^{-1}$ | Eq. (9) |

| | | | | |
|---|---|---|---|---|
| $m_{p,0}$ | Mortality constant | 0.008 | L ($\mu$g C)$^{-1}$ d$^{-1}$ | [34] |
| $\beta$ | Reduction in grazing due to toxin | $1.147 \times 10^5$ | cells ($\mu$g N)$^{-1}$ | Calibrated |
| | **Synthesis and growth** | | | |
| $J_{tot}$ | Total available C flux | - | $\mu$g C d$^{-1}$ | Eq. (6) |
| μ | Division rate of algae | - | d$^{-1}$ | Eq. (7) |
| $r$ | Growth rate of algae | - | d$^{-1}$ | Eq. (8) |
| $Q_{CN}$ | C:N mass ratio | 5.68 | $\mu$g C ($\mu$g N)$^{-1}$ | [51] |
| $Q_{CP}$ | C:P mass ratio | 41 | $\mu$g C ($\mu$g P)$^{-1}$ | [51] |

**Figures**

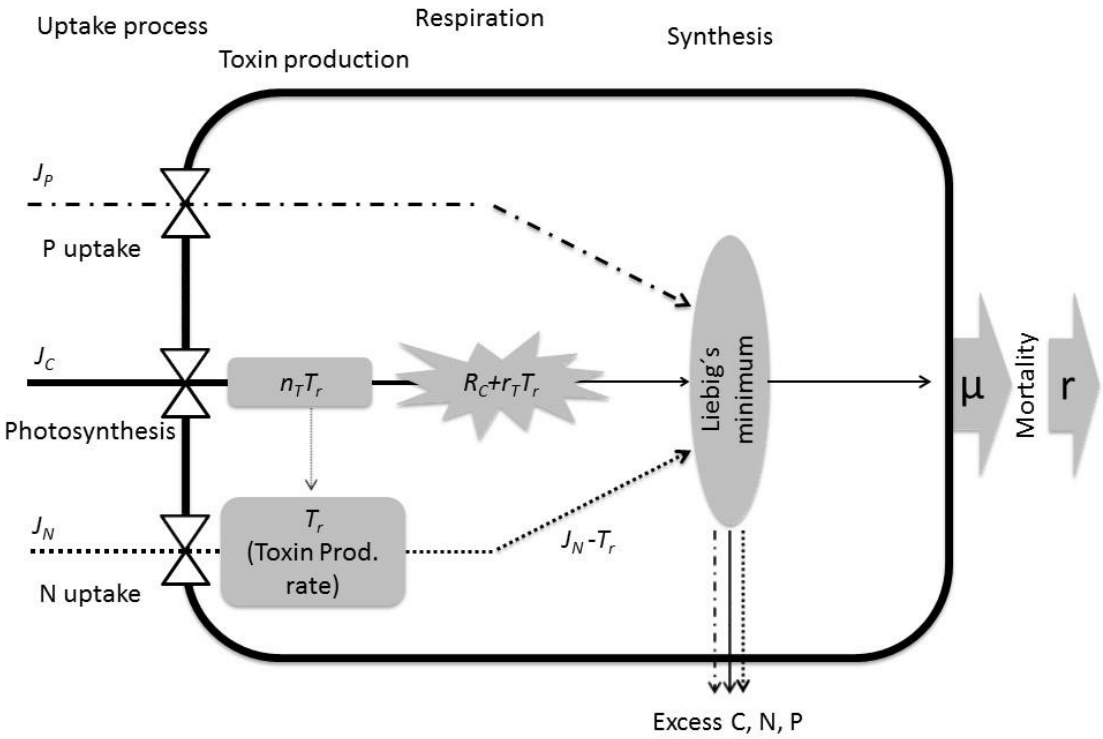


543

544 **Figure 1.** Schematic representation of the model showing how fluxes of nitrogen
545 (dotted), carbon (solid) and phosphorous (dash-dot) are lost through respiration (gray
546 explosion) and toxin production (gray rectangles), and combined (gray ellipse) to
547 determine growth rate. White triangle symbols represent the functional responses for
548 the uptake mechanisms. $R_C$ represents the respiratory cost that includes the costs of
549 both uptake and mobilization of resources for synthesis and the maintenance of
550 structure. The rate at which toxin is synthesized from C and N is $n_T T_r$, and the
551 respiratory cost of toxin production is $r_T T_r$ where $T_r$ is the toxin production rate. The
552 ellipse represents synthesis of biomass from the available C, N and P following
553 Liebig's law of the minimum and constrained by the Redfield ratio ($\mu$g C ($\mu$g N)$^{-1}$
554 =5.68, $\mu$g C ($\mu$g P)$^{-1}$=41) [51]. In our steady state consideration, the excess amounts
555 of assimilated C, N or P are assumed lost as excess resources. μ represents the

division rate, and $r$ is the population growth rate after subtracting predation mortality from μ.

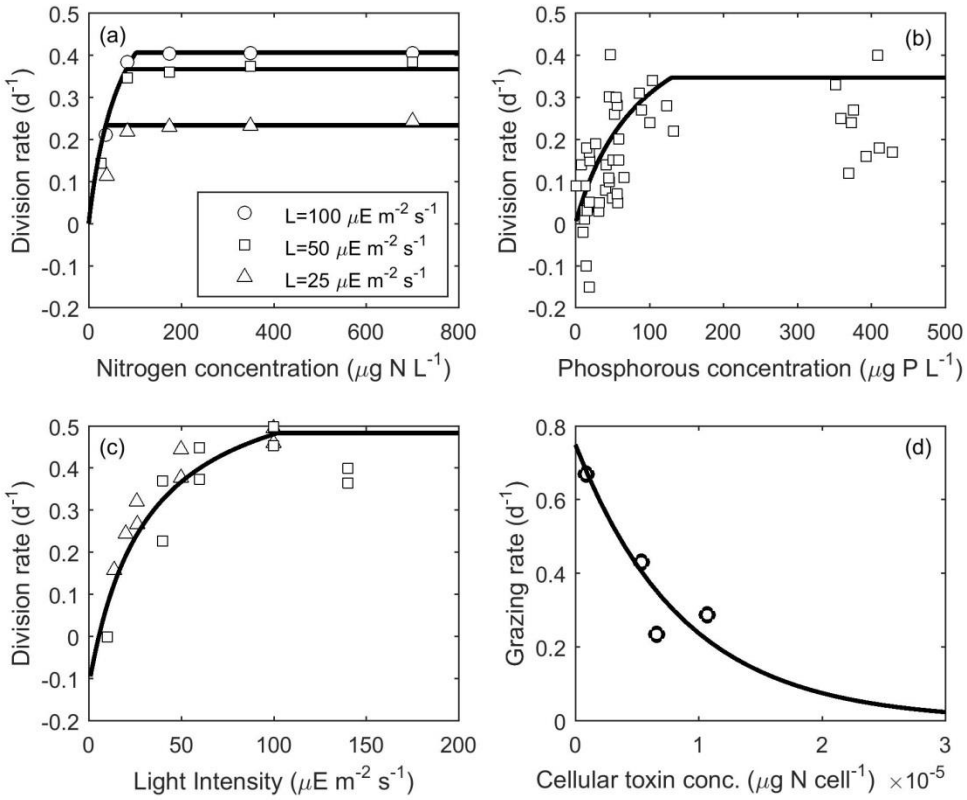


**Figure 2.** Comparison of division rates ($\mu$) between available data and model outcome with the calibrated parameters by varying (a) nitrogen ($P = 200$ $\mu$g P $L^{-1}$) (at three different light intensities $L =$ 100 $\mu$E $m^{-2}s^{-1}$, 50 $\mu$E $m^{-2}s^{-1}$, 25 $\mu$E $m^{-2}s^{-1}$) [52], (b) phosphorous ($L =$ 45 $\mu$E $m^{-2}s^{-1}$, $N = 200$ $\mu$g N $L^{-1}$) [53], and (c) light ($N = 6000$ $\mu$g N $L^{-1}$, $P =$ 400 $\mu$g P $L^{-1}$) [52, 54]. Grazing rate at different toxin concentrations (d). Data for grazing on toxic *A. tamarense* strain CCMP 115 by *A. tonsa* were used [12].

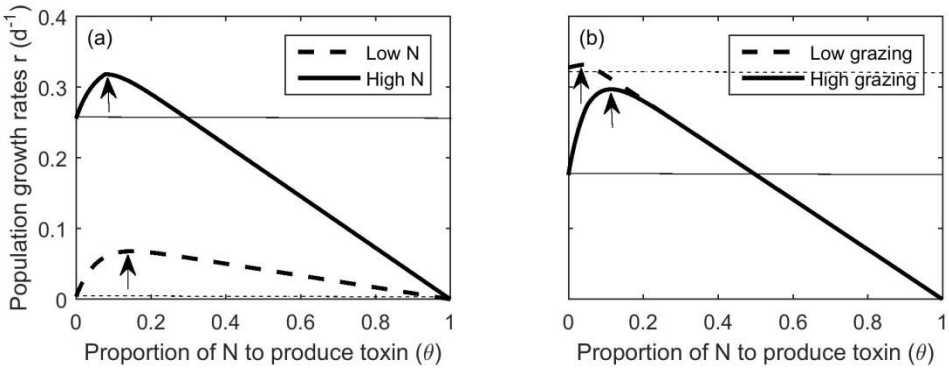


566

567 **Figure 3.** Population growth rate as a function of the fraction of assimilated nitrogen
568 that is allocated to toxin production (a) at low and high environmental concentration
569 of N (N=80 $\mu$g N $L^{-1}$ and 10 $\mu$g N $L^{-1}$ with concentration of grazer $Z = 10$ $\mu$g C $L^{-1}$),
570 and (b) at high and low concentration of zooplankton ($Z = 20$ $\mu$g C $L^{-1}$ and
571 1 $\mu$g C $L^{-1}$ with $N = 75$ $\mu$g N $L^{-1}$). The maximum of the curves shows the optimal
572 allocation strategy ($\theta$*) (marked by arrows). Thin lines represent growth rates in the
573 absence of toxin production. Other resources are phosphate (P) = 120 $\mu$g P $L^{-1}$, light
574 intensity (L) = 150 $\mu$E $m^{-2}s^{-1}$, and phytoplankton biomass (X) = 90 $\mu$g C $L^{-1}$.

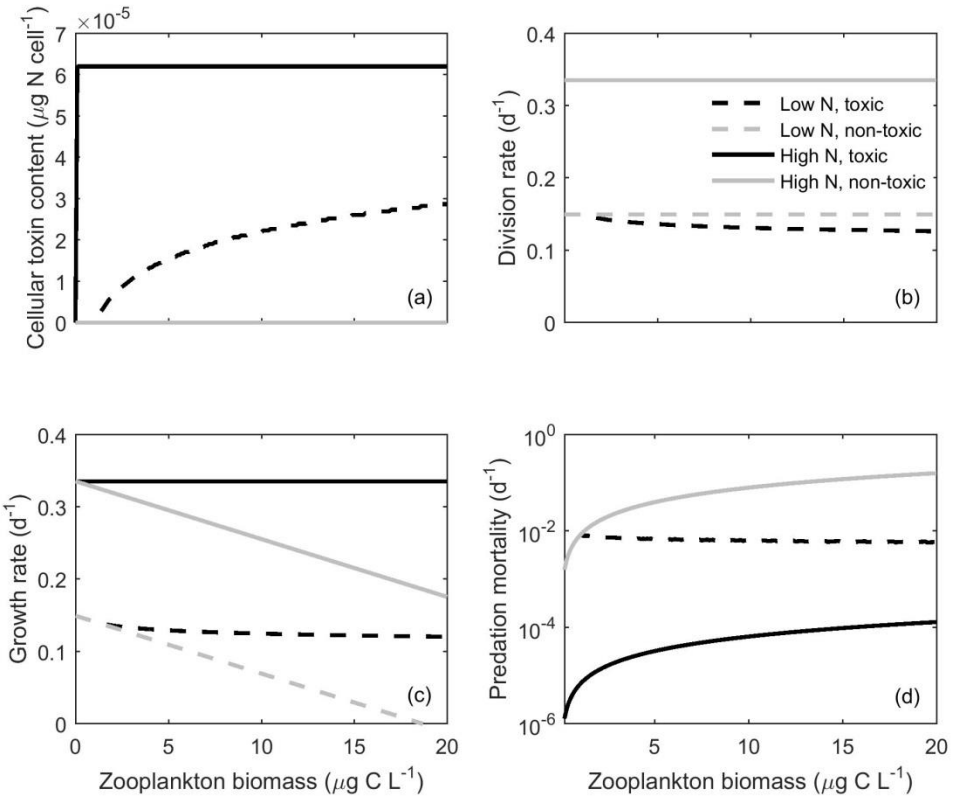


575

576 **Figure 4.** Optimal cellular toxin content (a), cell division rate (b), population growth
577 rate (c), and predation mortality (d) as a function zooplankton biomass at low (N=20
578 $\mu$g N $L^{-1}$) and high (N=150 $\mu$g N $L^{-1}$) N concentrations of defended (toxin producing)
579 and undefended cells (non-toxic strain). Curves of division rates for defended and
580 undefended cells under high N concentration lie on top of each other. Light intensity
581 $L = 150\ \mu\text{E m}^{-2}\text{s}^{-1}$ and phosphorous concentration $P = 120\ \mu\text{g P L}^{-1}$ in all plots.

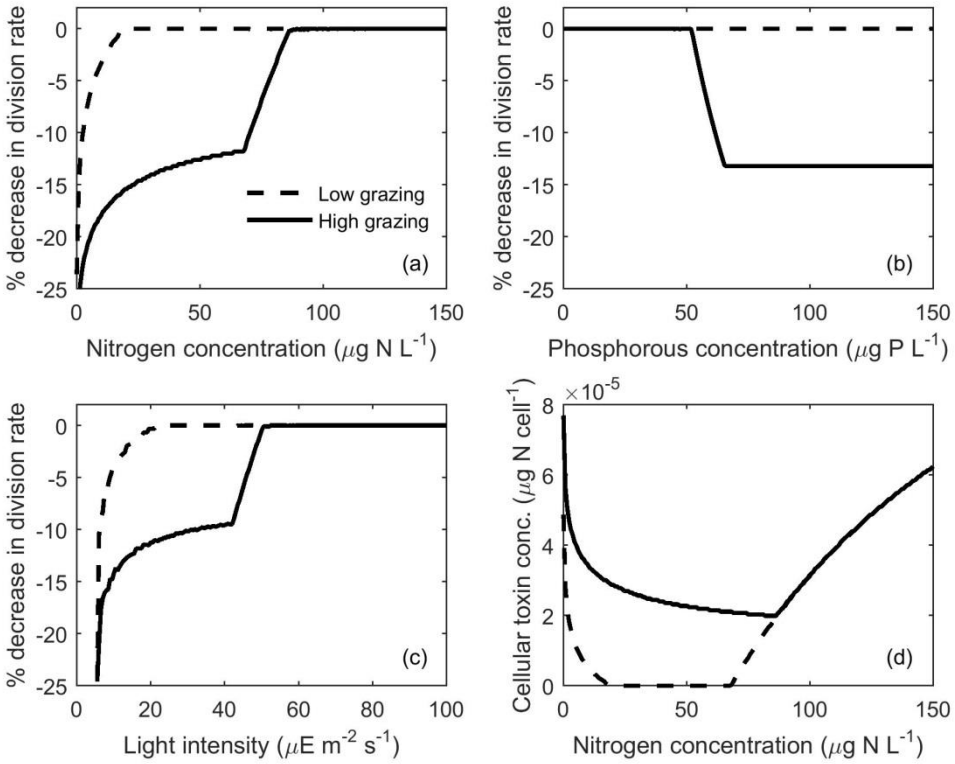


582

583 **Figure 5.** Relative reduction in cell division rate as a function of nitrogen
584 concentration (L=150 $\mu$E $m^{-2}s^{-1}$, P=120 $\mu$g P $L^{-1}$) (a), phosphorous concentration
585 (L=150 $\mu$E $m^{-2}s^{-1}$, N=40 $\mu$g N $L^{-1}$) (b), and light intensities (N=120 $\mu$g N $L^{-1}$,
586 P=120 $\mu$g P $L^{-1}$) (c) at high (Z=20 $\mu$g C $L^{-1}$) and low (Z=1 $\mu$g C $L^{-1}$) zooplankton
587 biomasses. Cellular toxin content as a function of N at high and low zooplankton
588 biomasses (d).

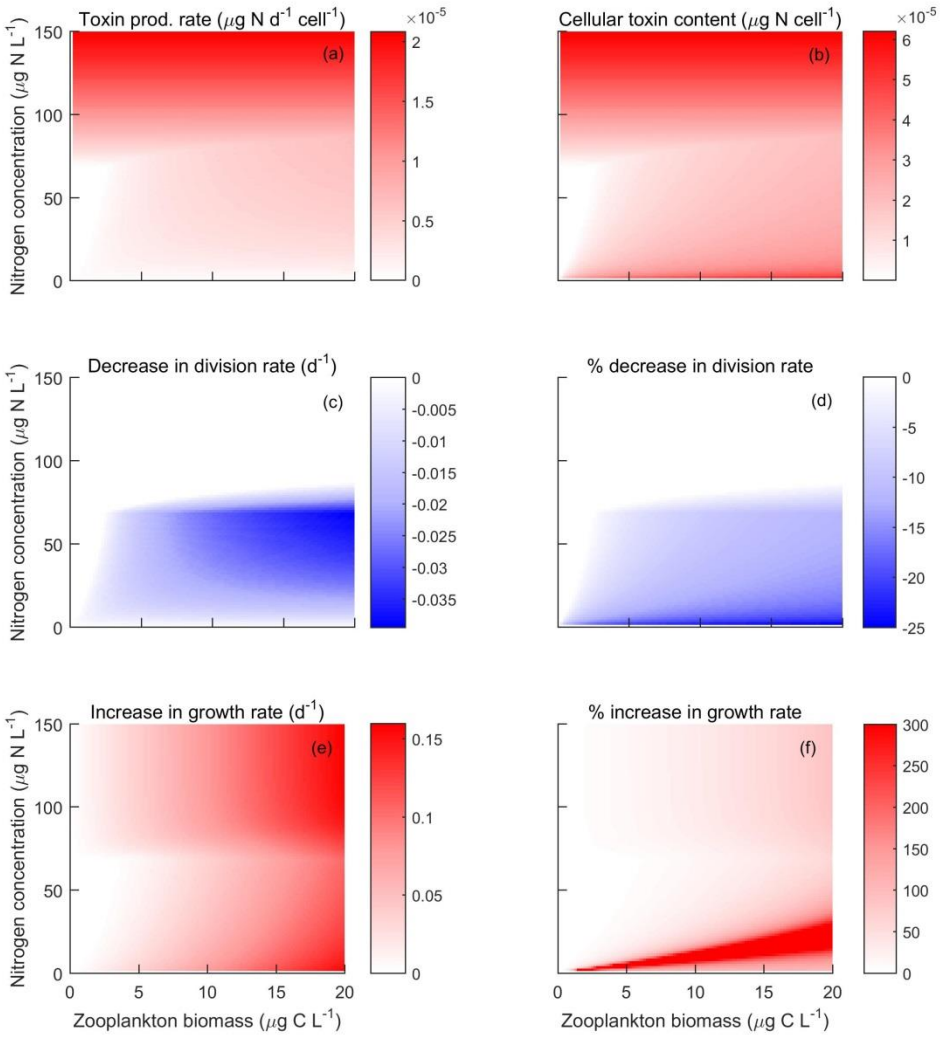


589

590 **Figure 6.** Surface plots of toxin production rate (a), and cellular toxin content (b), as
591 well as absolute and relative changes in cell division rate ($\mu(\theta^*) - \mu(\theta = 0)$ and
592 $(\mu(\theta^*) - \mu(\theta = 0)) \times 100/\mu(\theta = 0)$) (c, d), and population growth rates
593 ($g(\theta^*) - g(\theta = 0)$ and $(g(\theta^*) - g(\theta = 0)) \times 100/g(\theta = 0)$) (e, f) of defended relative
594 to undefended cells as a function of N-availability and zooplankton biomass. Light
595 intensity $L = 150\ \mu\text{E m}^{-2}\text{s}^{-1}$ and phosphorous concentration $P = 120\ \mu\text{g P L}^{-1}$ in
596 all plots.

597

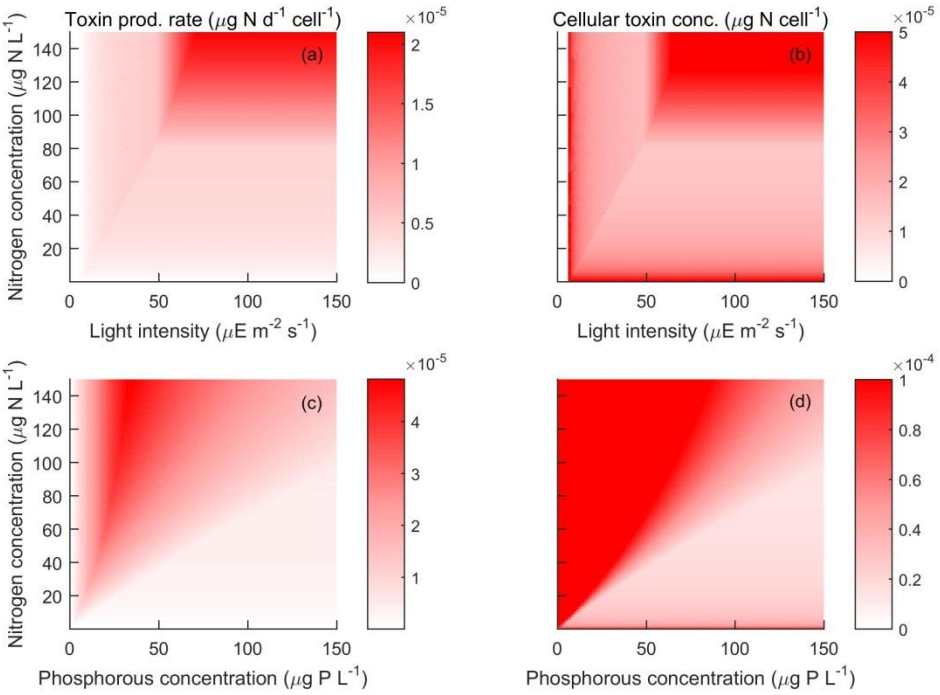


598

599 **Figure 7.** Surface plots of toxin production rate (a), and cellular toxin content (b) as a
600 function of N-availability and light intensity. Zooplankton biomasses Z=10 $\mu$g C $L^{-1}$,
601 and phosphorous concentration P=120 $\mu$g P $L^{-1}$ in both plots. Surface plots of toxin
602 production rate (c), and cellular toxin content (d) as a function of N and P-availability.
603 Zooplankton biomasses Z=10 $\mu$g C $L^{-1}$, and light intensity L=150 $\mu$E $m^{-2}s^{-1}$ in both
604 plots.

605

606

607

608

609

610

**Supplementary material**

**Appendix A.** Sensitivity analysis

Fig. A1 shows the color plot with continuous variations in both N concentration and the benefit from toxin production ($\beta$). The toxin production rate is high when the benefit from toxin production remains within certain range. However, it decreases at very high benefit range as organisms receive large benefit by producing small amount of toxin (Fig. A1b). As a result, benefits of toxin production in terms of population growth rate remains high when benefits are high and also N concentration is high.

Fig. A2 shows the color plot with continuous variations in both N concentration and the metabolic cost of synthesizing toxin ($r_T$). When the cost is relatively low, an increase in N concentration increases toxin production (Fig A2b), as organisms get more benefit from toxin production rather than increasing division rate. However, when the toxin production is costly and N is sufficient in the system, organisms invest their energy in increasing division rate rather than production of costly toxin. Although, since low N does not support high growth, organisms produce toxin to increase their population growth rate in spite of their high cost.

**Figure legends**

**Figure A1.** Surface plots of optimal allocation of N to toxin production (a), toxin production rate (b), and cellular toxin content (c), as well as absolute and relative changes in cell division rate (($\mu(\theta^*) - \mu(\theta = 0)$ and ($\mu(\theta^*) - \mu(\theta = 0)$)×100/$\mu(\theta = 0)$)) (d, e), and population growth rates (($g(\theta^*) - g(\theta = 0)$ and ($g(\theta^*) - g(\theta = 0)$)×100/$g(\theta = 0)$)) (f, g) of defended relative to undefended cells as a function of N-availability and the strength of toxicity ($\beta$). The position of arrow indicates the value of $\beta$ used for other figures. The phytoplankton biomasses X=90 $\mu$g C $L^{-1}$, zooplankton biomasses Z=10 $\mu$g C $L^{-1}$, light intensity L=150 $\mu$E $m^{-2}s^{-1}$, and phosphorous concentration P=120 $\mu$g P $L^{-1}$ in all plots.

**Figure A2.** Surface plots of optimal allocation of N to toxin production (a), toxin production rate (b), and cellular toxin content (c) as well as absolute and relative changes in cell division rate (($\mu(\theta^*) - \mu(\theta = 0)$ and ($\mu(\theta^*) - \mu(\theta = 0)$)×100/$\mu(\theta = 0)$)) (d, e) and population growth rates (($g(\theta^*) - g(\theta = 0)$ and ($g(\theta^*) - g(\theta = 0)$)×100/$g(\theta = 0)$)) (f, g) of defended relative to undefended cells as a function of N-availability and the cost of toxin production ($r_T$). The position of arrow indicates the value of $r_T$ used for other figures. The phytoplankton biomasses X=90 $\mu$g C $L^{-1}$, zooplankton biomasses Z=10 $\mu$g C $L^{-1}$, light intensity L=150 $\mu$E $m^{-2}s^{-1}$, and phosphorous concentration P=120 $\mu$g P $L^{-1}$ in all plots.

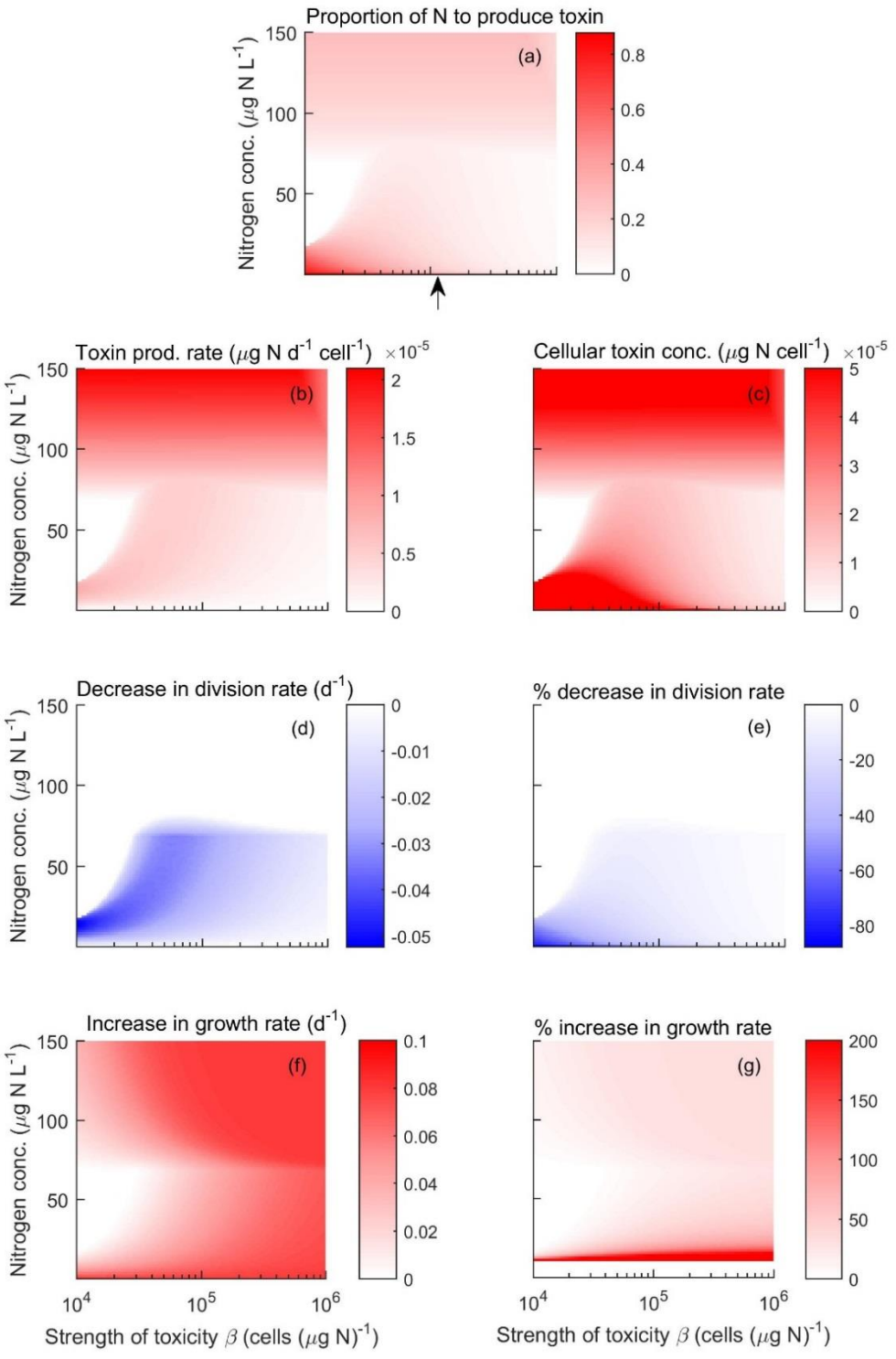


654

655 Figure A1

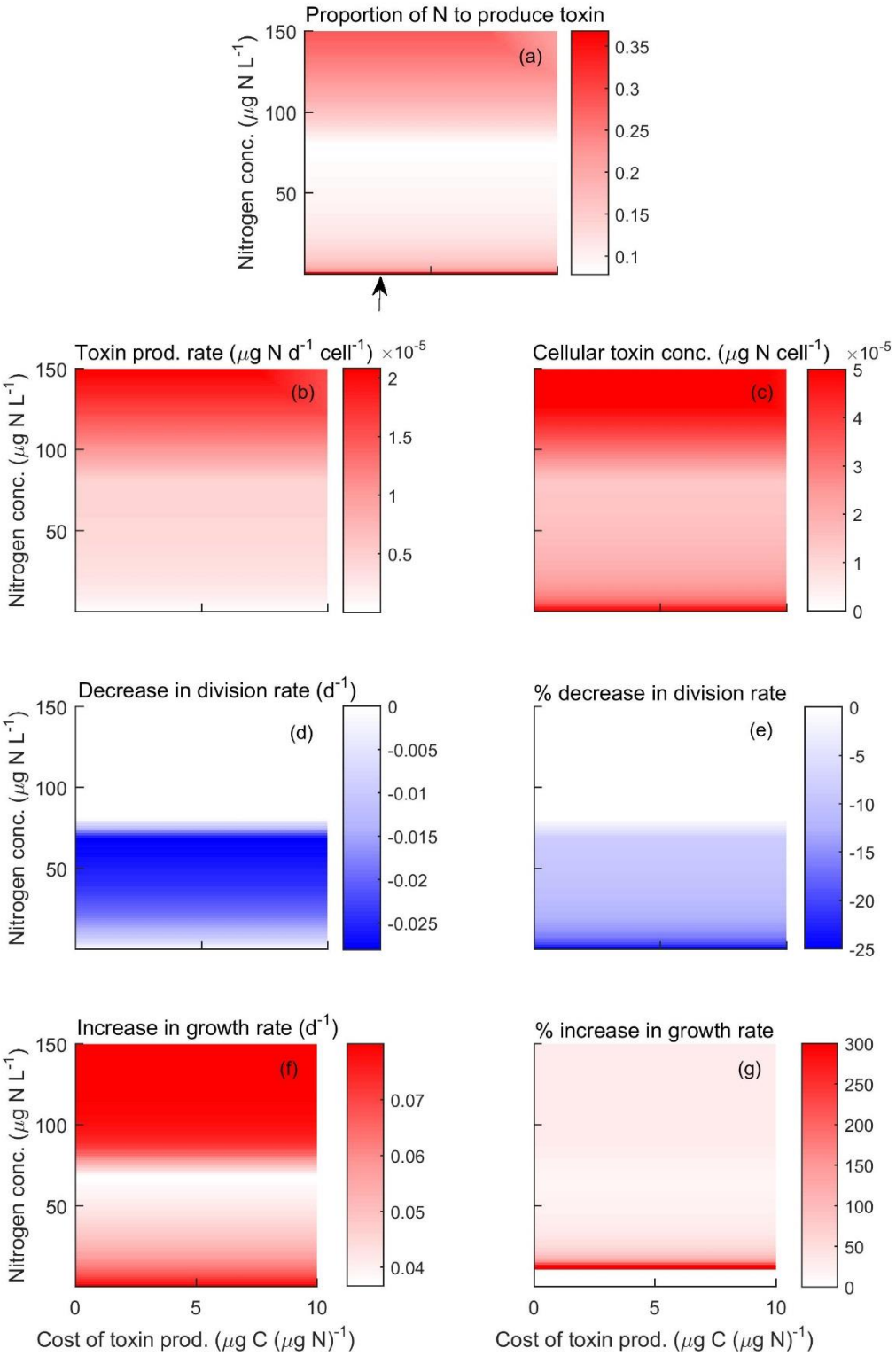


656
657 Figure A2

658